Progress In Electromagnetics Research C, Vol. 90, 65–77, 2019

Higher Order Mode Layered Cylindrical Dielectric Resonator Antenna

Abdulmajid A. Abdulmajid and Salam Khamas*

Abstract—A wideband high gain circularly polarized layered cylindrical dielectric resonator antenna (DRA) that operates in a higher order mode is proposed in the X-band frequency range. The antenna consists of two dielectric layers having different dielectric constants and radii. The results demonstrate a considerably improved performance as a result of adding the outer dielectric layer, where wider impedance and axial ratio bandwidths have been attained in conjunction with a higher broadside gain of $\sim$ 14 dBic. A prototype has been built and measured with close agreement between experimental and simulated results.

1. INTRODUCTION

The applications of cylindrical dielectric structures as resonant cavities were proposed more than five decades ago [1]. Since then, numerous studies have investigated their applications as high frequency radiators [1–6]. Compared with linearly polarized antennas, circularly polarized (CP) radiators offer a number of useful features such as eliminating the need for a precise alignment between transmitting and receiving antennas as well as a minimized impact of interference. Therefore, considerable studies have focused on the design of circularly polarized cylindrical DRAs. For example, a cross-slot fed CP cylindrical DRA that operates at the $HE_{11\delta}$ resonance mode has been reported with respective impedance and axial ratio (AR) bandwidths of 28% and 7.4% as well as a gain of $\sim$ 3.5 dBic at 5.75 GHz [7]. An alternative approach has been proposed in [8], where a cylindrical DRA that is fed by a number of slot apertures has been optimized to provide a comb-shape with an AR bandwidth of $\sim$ 4% and a 3.5 dBic gain. Furthermore, a CP cylindrical DRA fed by a quadruple strip has been investigated experimentally, where four vertical conformal strips have been placed around the DRA circumference in order to achieve wider AR and impedance bandwidths of 25.9% and 34.5%, respectively, in conjunction with a broadside gain of 5 dBic [9]. In another study, a single probe feeding has been utilized to excite several CP cylindrical and rectangular DRAs, where it has been noted that two orthogonal resonance modes, TM^x_{110} and TM^y_{110}, can be excited by changing the probe length to achieve maximum AR and impedance bandwidths of 1.2% and 5.7%, respectively [10]. Additionally, a study of a dual-band CP cylindrical DRA that operates in the HE_{111} and HE_{113} resonance modes have been presented with respective impedance and AR bandwidths of 23.5% and 7.4% and a maximum gain of 7 dBic [11]. In addition, respective impedance and axial ratio bandwidths of 25.36% and 3.23% have been achieved in conjunction with a 6.5 dBic gain using a single probe excitation of an elliptical cylindrical DRA [12]. Therefore, circularly polarized DRAs have been reported with a maximum broadside gain of 7 dBic for DRAs that support lower order resonance modes. However, a substantially higher gain can be accomplished by utilizing a DRA that operates in a higher order mode, albeit with a narrower bandwidth [13, 14].

Received 28 November 2018, Accepted 16 January 2019, Scheduled 19 February 2019
* Corresponding author: Salam Khamas (s.khamas@sheffield.ac.uk).
The authors are with the Department of Electrical Engineering and Electronics, University of Sheffield, Sheffield S1 4DT, UK.

The bandwidth enhancement of lower order mode operating cylindrical DRAs has received considerable attention by employing novel techniques such as introducing air gaps and DRA stacking, as well as coating, using various materials. For example, the first experimental results for a multi-layer wideband cylindrical DRA have been reported with an impedance bandwidth of 30% that has been achieved when the outer layer dielectric constant is approximately half that of the inner layer [15]. Additionally, a wider impedance bandwidth of 66% has been achieved in conjunction with a 5.5 dBi gain for a stacked cylindrical DRA that consists of three segments placed on top of each other with respective dielectric constants of 6.15, 2.32 and 10.2 for the bottom, middle and top layers [16]. In a later study, a wideband four-element cylindrical DRA array has been proposed with 47% impedance bandwidth and ~ 4 dBi gain, where the $TM_{01\delta}$ mode has been excited [17]. An alternative investigation has demonstrated that a substantial bandwidth enhancement can be achieved by stacking two cylindrical DRAs vertically [18], where a 55% impedance bandwidth and 5 dBi gain have been obtained. In addition, a wideband two-layer transparent cylindrical DRA has been demonstrated experimentally, here a conformal conducting strip has been utilized in order to excite the $HE_{11\delta}$ mode with 30% impedance bandwidth and 7 dBi gain [19]. A multilayer multi-permittivity half-cylindrical DRA has been investigated experimentally with more than 52% impedance bandwidth [20, 21].

Therefore, the reported layered cylindrical DRA studies have focused on the impedance bandwidth enhancement of linearly polarized lower order mode configurations. This mean far field radiation characteristics such as the axial ratio have not been considered for layered DRAs. In addition, a high gain wideband cylindrical DRA has not been reported in earlier studies neither for linearly nor circularly polarized radiations. Furthermore, the impact of the outer dielectric layer on higher order mode operation of cylindrical DRAs has also not been considered earlier. These limitations are addressed in this study where a layered higher order mode cylindrical DRA is proposed with noticeable improvement in the near and far field radiation characteristics. Experimental and simulated results demonstrate a broadside gain of approximately 14 dBic in combinations with wider axial ratio and impedance bandwidths. Additional advantages of incorporating the outer dielectric layer have been observed such as the enhanced tolerance to fabrication errors as was well as the improved physical support to otherwise a fragile DRA geometry due to a decreased aspect ratio. The proposed high-gain and wide-band antenna can be suitable for X-band applications such as satellite communication.

2. ANTENNA CONFIGURATION

The proposed layered cylindrical DRA and feed network are illustrated in Fig. 1, where the DRA dimensions have been chosen as $a_1 = 3$ mm, $h_1 = 32$ mm, $h_2 = 33$ mm with a variable outer layer thickness of δ_a. The antenna has been placed on a $150 \times 100\,\text{mm}^2$ ground plane that has been printed

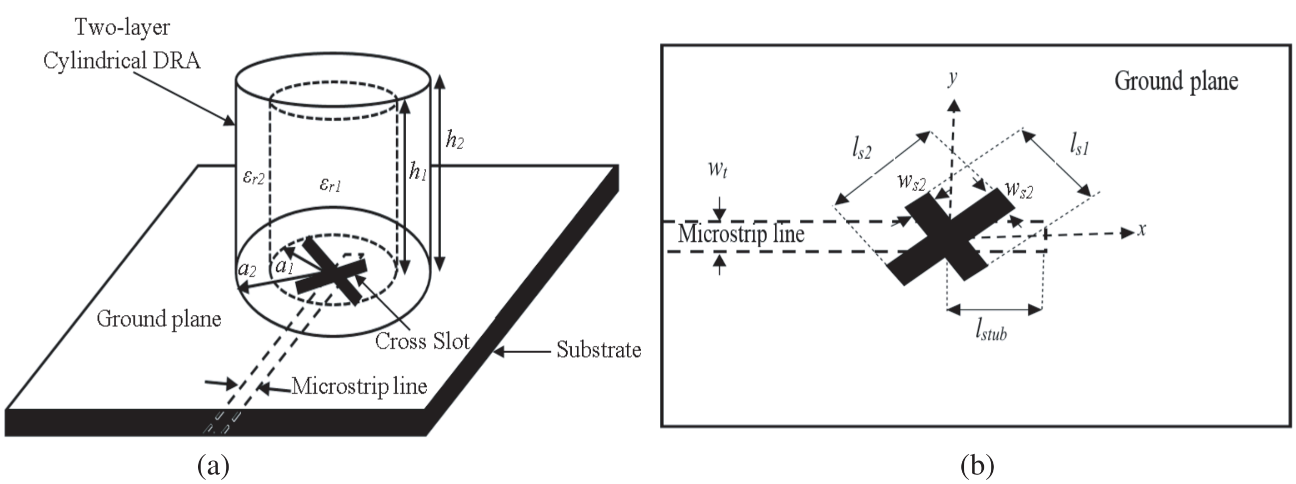

Figure 1. Geometry of the configuration. (a) Layered cylindrical DRA. (b) Top view of the feed network.

on a thin Ro4350B dielectric substrate with respective thickness, dielectric constant and loss tangent of 0.8 mm, 3.5 and 0.0037. The DRA element has been created using Alumina with a dielectric constant of 10 and loss tangent 0.0001, while the outer dielectric layer has been 3D printed using Polyimide with a dielectric constant of 3.5 and a loss tangent of 0.0027. Further, in order to generate CP radiation, a cross-slot has been itched on the ground plane with identical arm widths of $ws_1 = ws_2 = 0.7$ mm and unequal arm lengths of $ls_1 = 4.4$ mm and $ls_2 = 6.2$ mm. The whole structure has been fed using a microstrip line that has been printed on the lower side of the Ro4350B dielectric substrate with an open stub length of $l_{\text{stub}} = 2.5$ mm for optimum matching. Unequal length of cross-slot arms have been chosen in order to excite two near-degenerate orthogonal modes of equal amplitude and 90° phase difference, which generates the required CP wave [7, 9, 22]. Prototypes of the cylindrical DRA and the outer layer are presented in Fig. 2.

The parametric sweep of CST microwave studio has been utilized in order to study the impact of varying the outer layer thickness in terms of impedance and AR bandwidths as well as gain as illustrated Fig. 3 and Table 1. From these results it can be observed that a thicker outer layer of $\delta_a = 17$ mm, provides a significant improvement in the impedance and axial ratio bandwidths, as well as gain, to 28.34%, 9.52% and 13.9 dBic, respectively, compared to 5.96%, 0.86%, and 6.6 dBic for a single layer configuration. The improved bandwidth can be attributed to the fact that the outer dielectric coat acts as a transition layer between the DRA and free space. This is in addition to the merged bandwidths due to multi-mode excitation at adjacent resonance frequencies. Similarly the gain has been improved

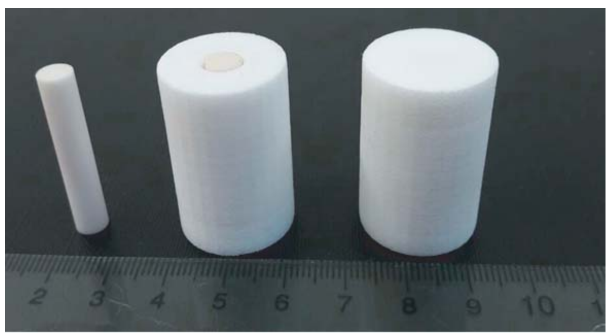

Figure 2. The outer dielectric coat and cylindrical DRA before and after assembly.

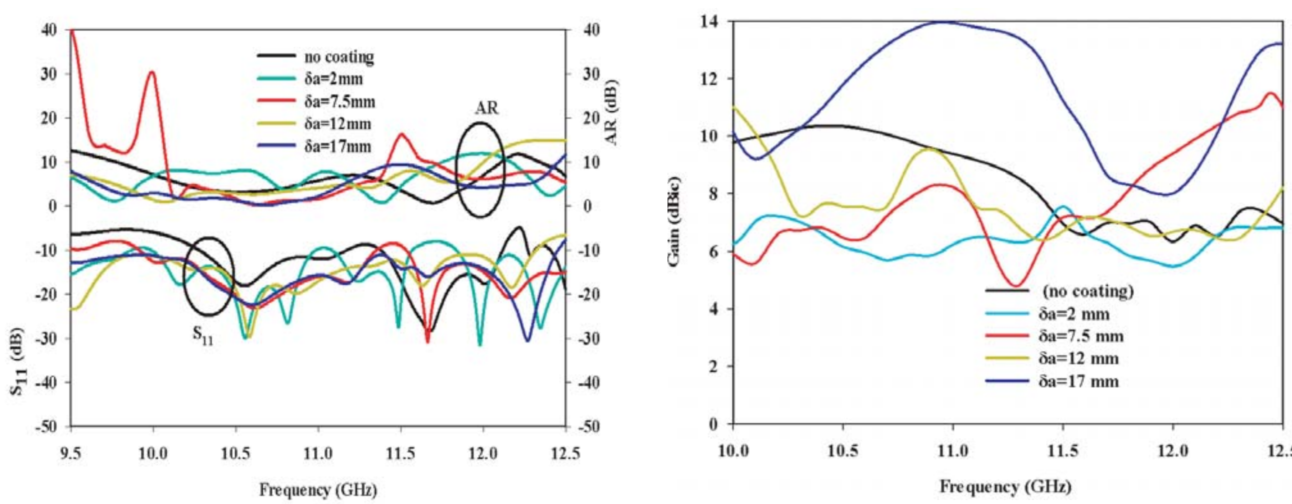

(a) (b)

Figure 3. Simulated characteristics of a two-layer circularly polarized cylindrical DRA for various δ_a. (a) S_{11} and AR. (b) Gain.

Table 1. Radiation characteristics for various outer layer radii when $a_1 = 3\,\text{mm}$.

$\delta(a_2 - a_1)$ mm	S_{11} bandwidth %	AR bandwidth %	Gain dBic
(no coating)	5.9	0.86	6.6
2 $(0.13\lambda_g)$	9.3	1.7	7.5
7.5 $(0.5\lambda_g)$	23.5	6.79	8.6
12 $(0.81\lambda_g)$	26.13	8.6	11
15 (λ_g)	28.34	8.8	12.27
17 $(1.14\lambda_g)$	28.34	9.52	13.9
23 $(1.5\lambda_g)$	28.24	3.2	9.6

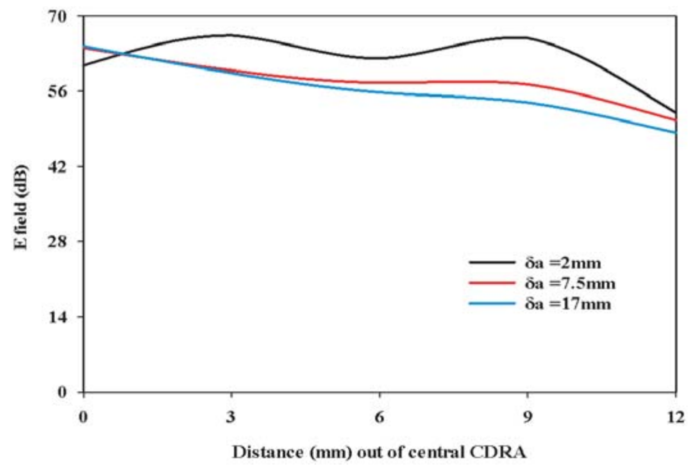

Figure 4. E-field strength around the circularly polarized layered cylindrical DRA at 11 GHz.

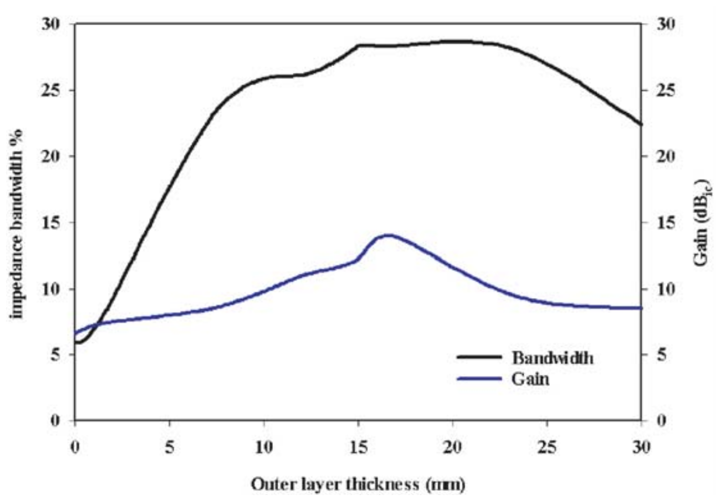

Figure 5. Impedance bandwidth and gain as functions of the outer layer thickness.

owing to multiple reasons such as exciting the higher order hybrid modes of HE_{117}, HE_{119} and $HE_{11,11}$ at 10 GHz, 10.6 GHz and 12 GHz, respectively, compared to only exciting the HE_{117} mode at 11.6 GHz for a single layer configuration. In addition, Fig. 4 demonstrates that increasing the outer layer thickness improves the energy confinement inside the dielectric resonator element resulting in a further gain increment. Moreover, with reference to Fig. 5, it can be noted that the maximum impedance and axial

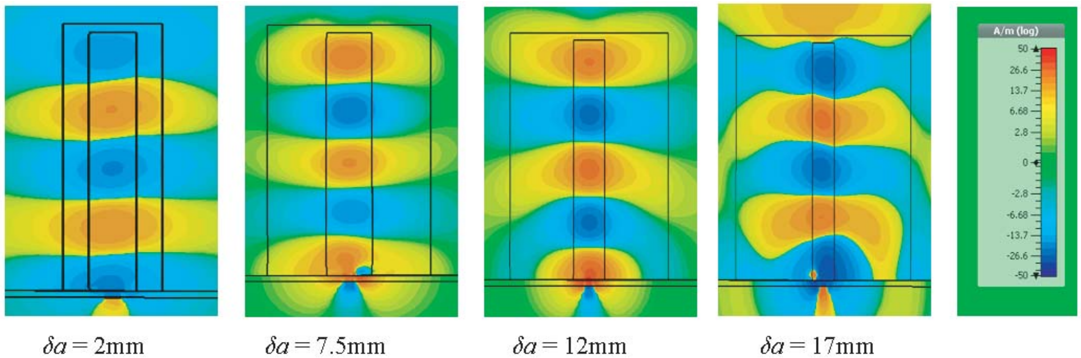

Figure 6. The H-field component inside a CP cylindrical DRA with varying outer layer thickness when the HE_{119} modes is excited at 10.6 GHz.

ratio bandwidths have been achieved in conjunction with a high gain using an outer layer thickness of $\delta_a = 17$ mm, which corresponds to $\sim 1.14\lambda_g$. The magnetic field distribution inside the CP CDRA is illustrated in Fig. 6 for various outer layer thicknesses at 10.6 GHz, where it can be noted that the excited higher order mode of HE_{119} has not been altered by varying the outer layer thickness. The impact of fabrication errors has also been investigated by studying the modes resonance frequency variation for fabrication errors of 0.05, 0.1 and 0.2 mm in the case of outer layer that has thicknesses of $\delta_a = 7.5$ and 17 mm. In each case the error has been added to the cylindrical DRA radius and the resonance frequency has been tracked for fixed coat dimensions. As can be noted from Table 2, the increment of the outer layer thickness minimizes the impact of fabrication errors. This can be attributed to the fact that for the layered CDRA, the dimensions variation is taking place in the vicinity of reduced wave reflections at the cylindrical DRA surface compared to the case of a single layer DRA, which means an improved fabrication tolerance.

Table 2. Impact of fabrication errors on the resonance frequency of the layered cylindrical DRA.

Fabrication error (mm)	Single layer CDRA (no coating) $\Delta f(\%)$	Two-layer CDRA ($\delta_a = 7.5$ mm) $\Delta f(\%)$	Two-layer CDRA ($\delta_a = 17$ mm) $\Delta f(\%)$
0.05	1.52	0.63	0.45
0.1	2.5	1.18	0.82
0.2	4.98	1.91	1.46

3. EXPERIMENTAL RESULTS

The inner cylindrical DRA has been fabricated by T-Ceram using Alumina with a fabrication precision of 0.05 mm. The outer dielectric layer has been printed with the aid of 3D printing technology at the University of Sheffield using Polyamide. Moreover, a double sided adhesive backed copper tape has been used in order to eliminate the air gaps between the antenna and ground plane. The DRA has been fed using an SMA connector that is connected in one end to the feeding microstrip line and in the other to the Agilent Technologies E5071C vector network analyzer thorough a 50 coaxial cable. The calibration has been implemented using the Agilents 85052D calibration kit. The radiation patterns and gain have been measured using an NSI near field system.

3.1. Single Layer Circularly Polarized CDRA Configuration

A single layer cylindrical DRA has been fabricated with dimensions that support the HE_{117} higher order mode. The reflection coefficient is presented in Fig. 7, and it can be noted that the respective simulated

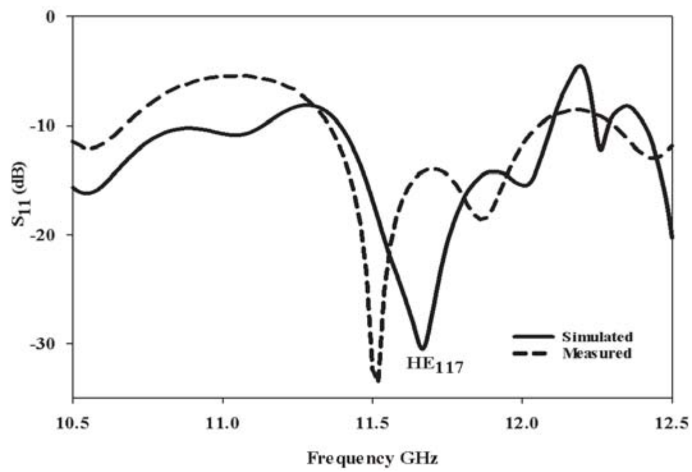

Figure 7. Reflection coefficient of a single-layer circularly polarized cylindrical DRA operating in the HE_{117} mode.

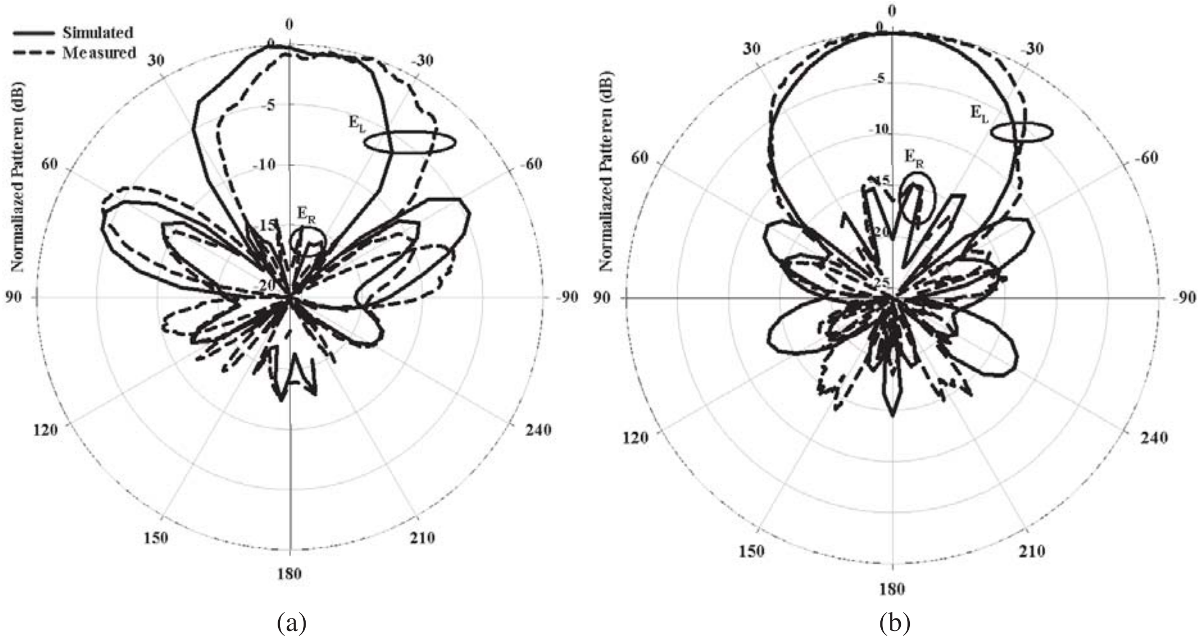

Figure 8. Radiation pattern of a single-layer circularly polarized cylindrical DRA excited in the HE_{117} mode at 11.55 GHz. (a) $\phi = 0°$. (b) $\phi = 90°$.

and measured impedance bandwidths are 6% and 5.8%, where the former extends from 11.4–12 GHz, and the latter covers a frequency range of 11.4–12 GHz. The slight discrepancy of 1% between experimental and simulated results can be attributed to measurements errors as well as a possible fabrication error of less than 0.2 mm as illustrated in Table 2. The simulated and measured radiation patterns for the HE_{117} mode, are illustrated in Fig. 8 at 11.55 GHz, where it can be noticed that this is a left-hand circularly polarized, LHCP, antenna since the broadside E_L component is stronger than the E_R counterpart by more than 15 dB. The measured and simulated AR and broadside gains are illustrated Fig. 9 with close agreement for a broadside gain of 6.6 dBic at 11.55 GHz. In addition, both of the simulated and measured axial ratio bandwidths are $\sim$ 0.86% over a frequency range of 11.5 to 11.6 GHz. Based on these results, it can be concluded that the narrower bandwidth represents a key limitation of higher order mode operation. Therefore, a layered CDRA will be considered next to accomplish gain and bandwidth enhancements at the same time.

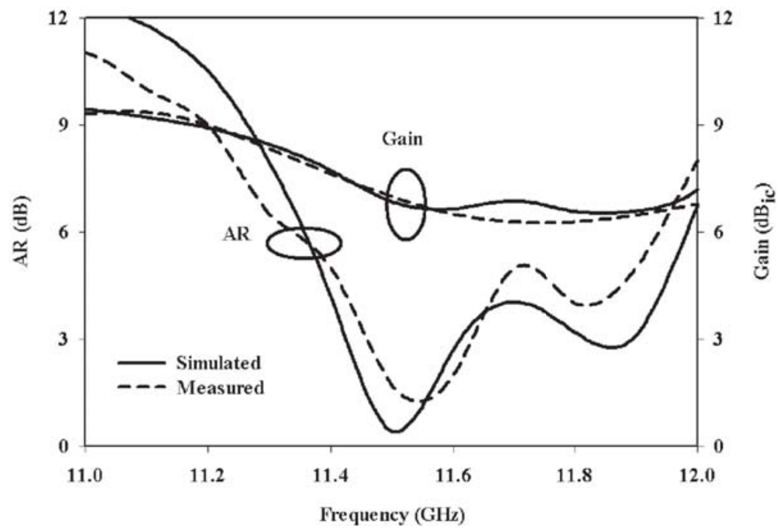

Figure 9. Gain and axial ratio of a single-layer circularly polarized cylindrical DRA.

3.2. Two Layer Circularly Polarized CDRA Configuration

The single layer cylindrical DRA has been coated by an outer dielectric layer fabricated using a 3D printing in order to address the narrower impedance and AR bandwidth limitations as well as improving the gain further. A cylindrical airgap with a radius of a_1 has been created in the center of the outer dielectric layer in order to accommodate the DRA element as illustrated in Fig. 2. Potential airgaps between the two cylindrical layers have been eliminated using a Polyamide dielectric powder. Although measurements have demonstrated a negligible airgaps impact at the considered frequency range, it is expected that such impact will be more pronounced at the mm-wave frequency range. Fig. l0 presents the simulated and measured return losses in the case of $\delta_a = 7.5\,\text{mm}$, where it can be observed that the simulated impedance bandwidth is 23.5%, which extends from 10–12.6 GHz, and agrees well with the measured counterpart of 22% over a frequency range of 10–12 GHz. The increment in the mode

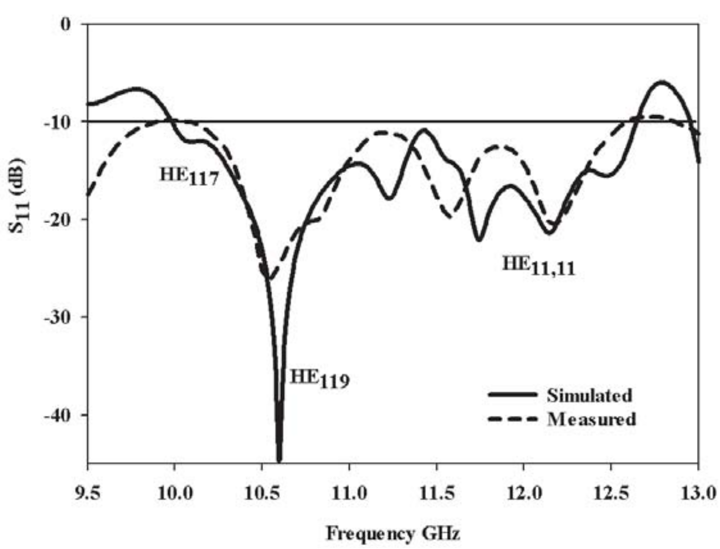

Figure 10. Reflection coefficient of a multi-layer circularly polarized cylindrical DRA when $\delta_a = 7.5\,\text{mm}$.

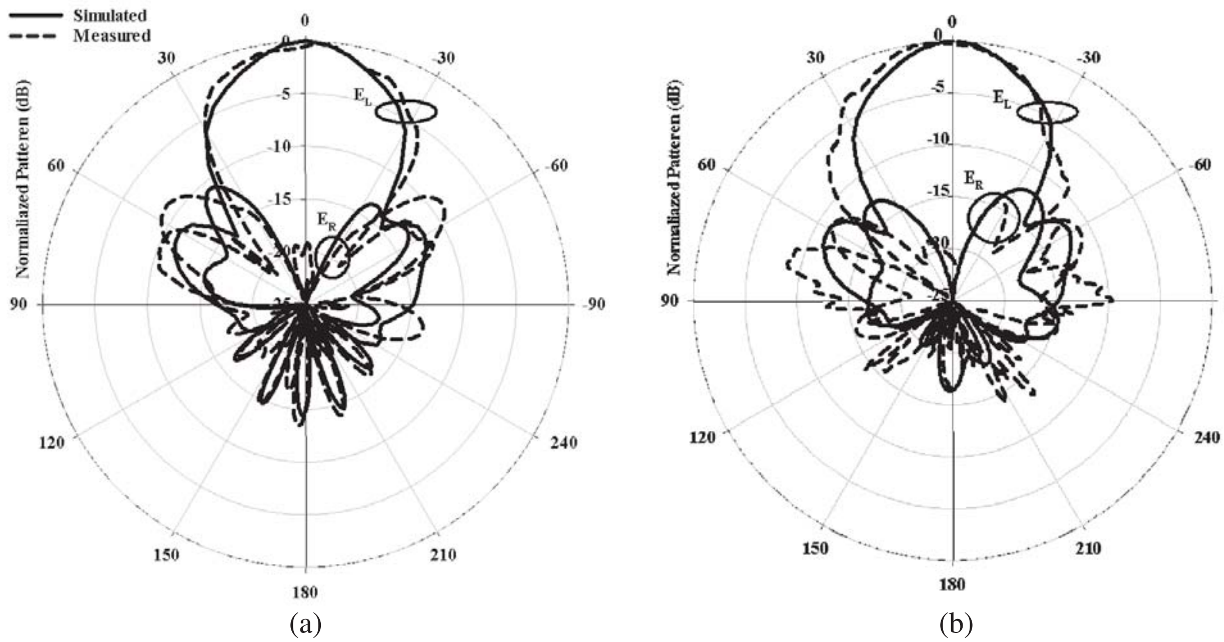

Figure 11. Radiation patterns of a multi-layer circularly polarized cylindrical DRA when $\delta_a = 7.5\,\text{mm}$ at 10.6 GHz. (a) $\phi = 0°$. (b) $\phi = 90°$.

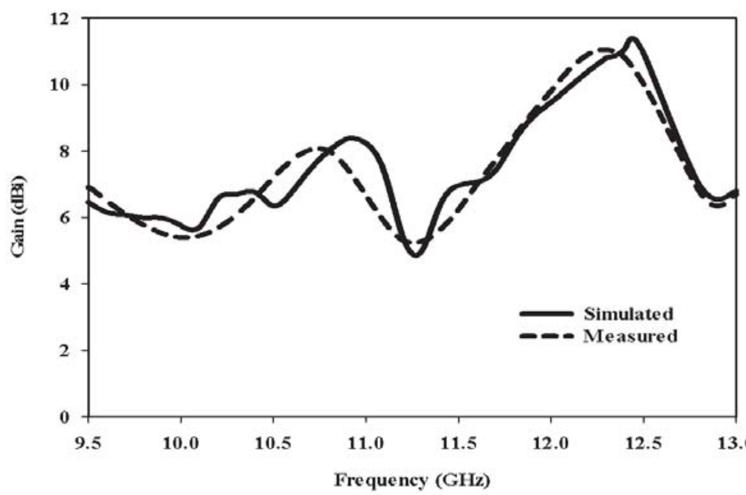

Figure 12. Gain of a multi-layer circularly polarized cylindrical DRA when $\delta_a = 7.5\,\text{mm}$.

order can be attributed to the increment of the permittivity of the surrounding medium [23]. Fig. 11 illustrates the radiation patterns for the HE_{119} mode at 10.6 GHz, where a LHCP radiation exists since the boresight E_L magnitude is greater than the E_R counterpart by more than 20 dB. Exciting the HE_{119} and $HE_{11,11}$ modes has contributed to increasing the antenna gain to 8.6 dBic for the HE_{119} mode and 11 dBi at the $HE_{11,11}$ resonance mode as shown in Fig. 12. The axial ratio has been simulated and measured at boresight as depicted in Fig. l3. The simulations predict a 3 dB AR bandwidth of 6.8% that extends from 10.4 to 11 GHz, which agrees well with the measured counterpart. The enhanced axial ratio bandwidth results from the merged bandwidths of the HE_{117} and HE_{119} resonance modes that have been excited at 10 and 10.9 GHz, respectively. These results demonstrate sound improvements in the higher order modes DRA performance when a dielectric coat layer is incorporated.

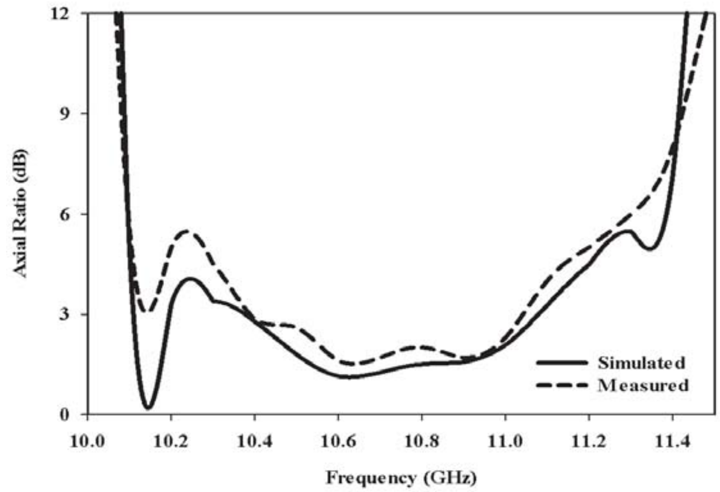

Figure 13. Axial ratio of a multi-layer circularly polarized cylindrical DRA when $\delta_a = 7.5\,\text{mm}$.

3.3. Further Performance Improvement

The antenna performance in terms of axial ratio and impedance bandwidths, as well as gain, can be improved further by altering the outer layer thickness. Therefore, a second optimized design has been measured using an outer dielectric layer thickness of $\delta_a = 17\,\text{mm}$. However, in order to maintain an optimum matching, the width of the cross-slot arms has been altered to $ws_1 = ws_2 = 0.8\,\text{mm}$ while the unequal slot arm lengths have not been modified. This variation in the slot width is expected as the effective dielectric constant of the configuration can be altered for various outer layer radii. Fig. 14 presents the simulated and measured reflection coefficients of the thicker circularly polarized layered CDRA, where it can be noted that the simulated impedance bandwidth of 28%, which covers a frequency range of 9.4–12.5 GHz, agrees well with the measured counterpart of 28.3% that extends from 9.3 to 12.3 GHz. Once again, the same higher order resonance modes of HE_{117}, HE_{119}, and $HE_{11,11}$ have been excited at 9.6, 10.6, and 12.2 GHz, respectively. The far field patterns are illustrated in Fig. 15 for the HE_{119} resonance mode at the minimum axial ratio frequency point of 10.6 GHz. The left-hand circularly polarized (LHCP) radiation has been maintained since the E_L field in the boresight direction is stronger

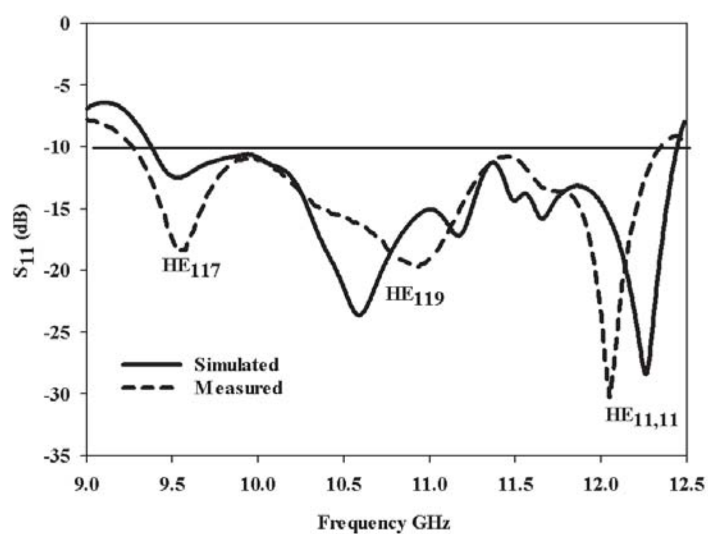

Figure 14. Reflection coefficient of circularly polarized layered cylindrical DRA when $\delta_a = 17\,\text{mm}$.

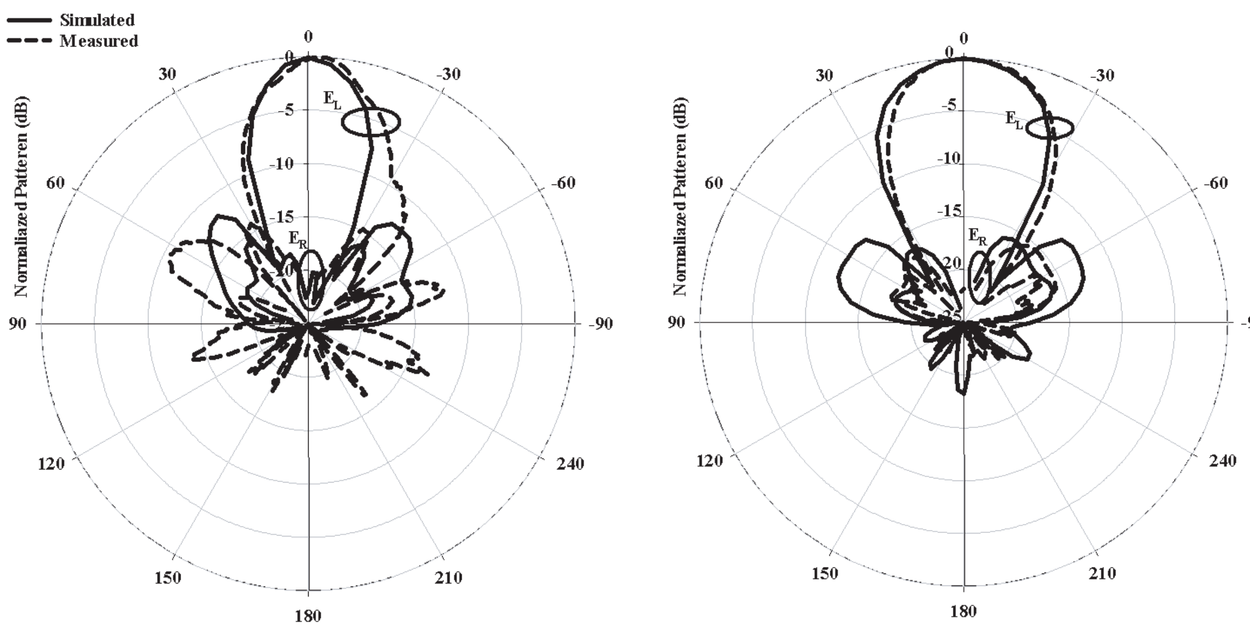

(a) (b)

Figure 15. Radiation pattern of a circularly polarized layered cylindrical DRA with an outer layer radius of $\delta a = 17\,\text{mm}$ excited in the HE_{119} mode at 10.6 GHz. (a) $\phi = 0°$. (b) $\phi = 90°$.

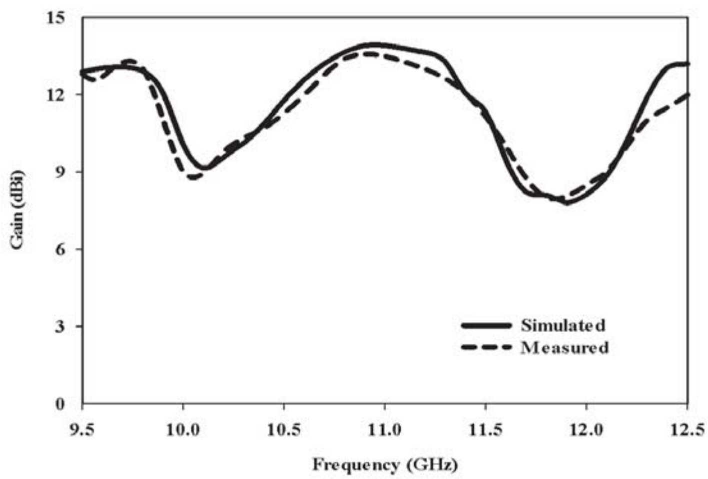

Figure 16. Gain of a circularly polarized layered cylindrical DRA with an outer layer radius of $\delta_a = 17\,\text{mm}$.

than the E_R component by more than 23 dB. It should be noted that the weaker electromagnetic fields inside the thicker outer layer minimizes the radiation to the DRA sides. In contrast, stronger confined fields exist inside the DRA element, which contributes to a maximized broadside radiation and, hence, higher gains of 13.9 dBic and 11.7 dBi for the HE_{119} and $HE_{11,11}$ resonance modes, respectively, as illustrated in Fig. l6. The simulated and measured axial ratios are presented in Fig. l7 with almost identical bandwidths of $\sim 9.5\%$ over a frequency range of 10 to 11 GHz. These results confirm that increasing the outer layer thickness, δ_a, from 7.5 to 17 mm, improves the gain from 8.6 to 13.9 dBic, respectively. As mentioned earlier, this enhancement can be attributed to the fact that increasing the thickness of the outer dielectric enhances the maximum energy confinement inside the dielectric

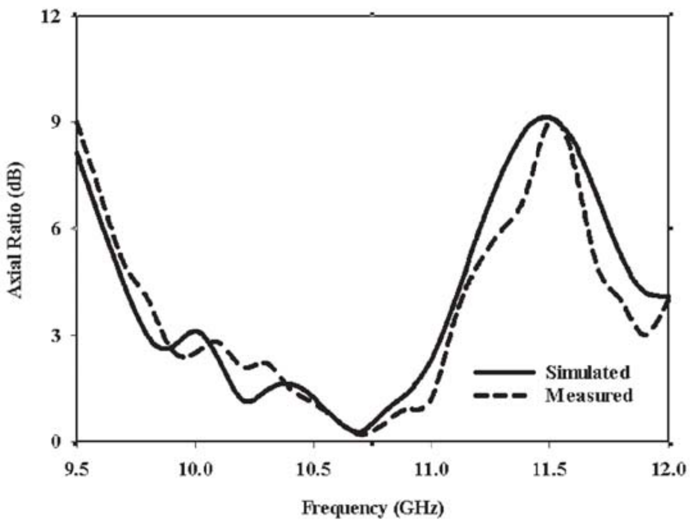

Figure 17. Axial ratio of a layered circularly polarized cylindrical DRA with an outer layer radius of $\delta_a = 17\,\text{mm}$.

Table 3. Comparison between the proposed layered circularly polarized cylindrical DRA and previously reported designs.

References	Impedance BW	AR BW	Outer layer size	Gain dBic	Resonance Mode	Feeding mechanism
Proposed antenna $\delta_a = 7.5\,\text{mm}$	23.5%	6.8%	$0.5\lambda_g$	8.6	HE_{119}	Cross slot
Proposed antenna $\delta_a = 17\,\text{mm}$	28.3%	9.5%	$1.14\lambda_g$	13.9	HE_{119}	Cross slot
[7]	28%	4.7%	-	3.5	$HE_{11\delta}$	Cross slot
[8]	9%	4%	-	3.5	-	Coaxial probe
[9]	34.5%	25.9%	-	5	-	strip feed
[10]	5.7%	1.8%	-	-	TM_{110}	probe
[11]	23.5%	7.4%	-	7	HE_{113}	Slot aperture
[12]	25.36 %	3.23%	-	6.5	-	probe
[24]	18%	-	$0.77\lambda_g$	-	$TM_{01\delta}$	probe
[25]	45%	-	$0.85\lambda_g$	-	$TM_{01\delta}$	probe

resonator layer.

Based on the presented analyses and results, increasing the outer layer thickness improves all the radiation characterises as well as fabrication tolerance. On the other hand, an outer layer thickness of $\delta_a = 17\,\text{mm}$ increases the antenna size considerably, which may not be appealing for applications at the considered frequency range. However, as the frequency increases, the physical antenna size will be substantially reduced. For example, at frequencies of 40 and 60 GHz, the inner DRA radii will be 0.9 and 0.6 mm, respectively, compared to respective heights of 9.6 and 6.4 mm. Such long and thin ceramic DRAs will be fragile and easy to break. At the same time, the thicker outer layer radii are 6 and 4 mm at 40 and 60 GHz, respectively. These thicknesses will provide a robust antenna structure with extra physical support while maintaining the particularly needed higher gain that represents the most important requirement from a mm-wave antenna. Finally, a comprehensive comparison between the proposed layered cylindrical DRA and the previously reported designs is summarised in Table 3, where it can be observed that the proposed antenna outperforms the published counterparts and offers appealing features such as the combination of wide impedance and axial ratio bandwidths, higher gain as well as an improved fabrication tolerance. It should be noted that this is the first antenna design that offers a combination of these attractive radiation characteristics.

4. CONCLUSION

Circularly polarized layered cylindrical DRAs have been considered theoretically and experimentally, where it has been demonstrated that incorporating an outer dielectric layer provides wider impedance and axial ratio bandwidths as well as high gain in a simple design. The two-layer circularly polarized cylindrical DRA operates in the HE_{119} mode and offer respective impedance and axial bandwidths of $\sim$ 28.3% and 9.5% in conjunction with a high gain of up to 13.9 dBic, which could have not been achieved at the absence of the outer dielectric coat. Increasing the impedance bandwidth by coating the antenna with a layer of lower permittivity is expected and have been reported in the literature. However, gain enhancement, wider axial ratio bandwidth, and improved fabrication tolerance have not been demonstrated earlier for a layered cylindrical DRA. Furthermore, two prototypes with outer layer thicknesses of $\delta_a = 7.5$ mm and 17 mm have been considered. The first demonstrates a design with practical dimensions for the X-band frequency range. On the other hand, the potential of the second design could be exploited further at higher frequencies, for example at 60 GHz where the outer layer radius will be reduced to 4 mm.

REFERENCES

1. Yee, H. Y., "Natural resonant frequencies of microwave dielectric resonators (correspondence)," *IEEE Transactions on Microwave Theory and Techniques*, Vol. 13, 256–256, 1965.
2. Long, S., M. McAllister, and L. Shen, "The resonant cylindrical dielectric cavity antenna," *IEEE Transactions on Antennas and Propagation*, Vol. 31, 406–412, 1983.
3. Kishk, A., B. Ahn, and D. Kajfez, "Broadband stacked dielectric resonator antennas," *Electronics Letters*, Vol. 25, 1232–1233, 1989.
4. Martin, J. S., Y. Antar, A. Kishk, A. Ittipiboon, and M. Cuhaci, "Dielectric resonator antenna using aperture coupling," *Electronics Letters*, Vol. 26, 2015–2016, 1990.
5. Shahine, M. A., M. Al-Husseini, K. Kabalan, and A. El-Hajj, "An ultra-wideband dielectric resonator antenna with reconfigurable band rejection," *PIERS Proceedings*, 534–537, Moscow, Russia, August 19–23, 2012.
6. Zainud-Deen, S. H., H. A. El-Azem Malhat, and K. H. Awadalla, "A single-feed cylindrical superquadric dielectric resonator antenna for circular polarization," *Progress In Electromagnetics Research*, Vol. 85, 409–424, 2008.
7. Almpanis, G., C. Fumeaux, and R. Vahldieck, "Offset cross-slot-coupled dielectric resonator antenna for circular polarization," *IEEE Microwave and Wireless Components Letters*, Vol. 16, 461–463, 2006.
8. Chu, L., D. Guha, and Y. Antar, "Comb-shaped circularly polarised dielectric resonator antenna," *Electronics Letters*, Vol. 42, 785–787, 2006.
9. Khoo, K.-W., Y.-X. Guo, and L. C. Ong, "Wideband circularly polarized dielectric resonator antenna," *IEEE Transactions on Antennas and Propagation*, Vol. 55, 1929–1932, 2007.
10. Malekabadi, A., M. H. Neshati, and J. Rashed-Mohassel, "Circular polarized dielectric resonator antennas using a single probe feed," *Progress In Electromagnetics Research C*, Vol. 3, 81–94, 2008.
11. Fang, X. S. and K. W. Leung, "Linear-/circular-polarization designs of dual-/wide-band cylindrical dielectric resonator antennas," *IEEE Transactions on Antennas and Propagation*, Vol. 60, 2662–2671, 2012.
12. Zainud-Deen, S. H., H. A. Malhat, and K. H. Awadalla, "Circular polarized dielectric resonator antenna for portable RFID reader using a single feed," *International Journal of Radio Frequency Identification & Wireless Sensor Networks*, Vol. 1, No. 1, 22–27, 2011.

13. Mrnka, M. and Z. Raida, "Enhanced-gain dielectric resonator antenna based on the combination of higher-order modes," *IEEE Antennas and Wireless Propagation Letters*, Vol. 15, 710–713, 2016.
14. Petosa, A. and S. Thirakoune, "Rectangular dielectric resonator antennas with enhanced gain," *IEEE Transactions on Antennas and Propagation*, Vol. 59, 1385–1389, 2011.
15. Shum, S. and K. Luk, "Numerical study of a cylindrical dielectric-resonator antenna coated with a dielectric layer," *IEE Proceedings — Microwaves, Antennas and Propagation*, Vol. 142, 189–191, 1995.
16. Huang, W. and A. Kishk, "Compact wideband multi-layer cylindrical dielectric resonator antennas," *IET Microwaves, Antennas and Propagation*, Vol. 1, 998–1005, 2007.
17. Chaudhary, R. K., K. V. Srivastava, and A. Biswas, "Four element multilayer cylindrical dielectric resonator antenna excited by a coaxial probe for wideband applications," *2011 National Conference on Communications (NCC)*, 1–5, 2011.
18. Maknikar, R. D. and V. G. Kasabegoudar, "Circularly polarized cross-slot-coupled stacked dielectric resonator antenna for wireless applications," *International Journal of Wireless Communications and Mobile Computing*, Vol. 1, 68–73, 2013.
19. Sun, Y., X. Fang, and K. W. Leung, "Wideband two-layer transparent cylindrical dielectric resonator antenna used as a light cover," *2015 IEEE International Conference on Computational Electromagnetics (ICCEM)*, 286–287, 2015.
20. Chaudhary, R. K., K. V. Srivastava, and A. Biswas, "Broadband four-element multi-layer multi-permittivity cylindrical dielectric resonator antenna," *Microwave and Optical Technology Letters*, Vol. 55, 932–937, 2013.
21. Chaudhary, R. K., K. V. Srivastava, and A. Biswas, "Variation of permittivity in radial direction in concentric half-split cylindrical dielectric resonator antenna for wideband application," *International Journal of RF and Microwave Computer-Aided Engineering*, Vol. 25, 321–329, 2015.
22. Huang, C.-Y., J.-Y. Wu, and K.-L. Wong, "Cross-slot-coupled microstrip antenna and dielectric resonator antenna for circular polarization," *IEEE Transactions on Antennas and Propagation*, Vol. 47, 605–609, 1999.
23. Abdulmajid, A. A., Y. Khalil, and S. K. Khamas, "Higher order mode circularly polarised two-layer rectangular dielectric resonator antenna," *IEEE Antennas and Wireless Propagation Letters*, Vol. 17, 1114–1117, 2018.
24. Shum, S. and K. Luk, "Stacked annular ring dielectric resonator antenna excited by axi-symmetric coaxial probe," *IEEE Transactions on Antennas and Propagation*, Vol. 43, 889–892, 1995.
25. Ong, S. H., A. A. Kishk, and A. W. Glisson, "Wideband disc-ring dielectric resonator antenna," *Microwave and Optical Technology Letters*, Vol. 35, 425–428, 2002.